Advanced Steel Construction – Vol. 22 No. 2 (2026) 143–152
DOI:10.18057/IJASC.2026.22.2.2

STUDY ON THE FATIGUE PERFORMANCE OF CROSS-WELDED STEEL FABRIC FOR SIMPLE-SUPPORTED BOX GIRDER OF HIGH-SPEED RAILWAY

Chuang Du *, Qi-Hui Gao, Jin-Li Qiao, Xiao-Tong Liu and Didier Nshimiyimana

School of Civil Engineering and Transportation, Hebei University of Technology, Tianjin 300401, China
** (Corresponding author: E-mail: duch_1@sina.com)*

ABSTRACT

By utilizing intelligent construction technology, the production process of the steel fabric for simply - supported box girders in high - speed railways has been upgraded from manual binding to automatic welding. However, welding can affect the fatigue performance of steel bars. To evaluate this impact, fatigue tests were conducted on five groups of specimens as well as the base metal. The test results indicate that fatigue failure occurred at the welded spot, presenting as a brittle failure. As the stress amplitude decreases, the fatigue life of the specimens increases significantly. The fatigue life is more sensitive to stress changes at low - stress amplitudes. When the stress ratio increases, both the fatigue life and the stress amplitude decrease, and the sensitivity of the fatigue life and stress amplitude to the stress ratio gradually increases. On the overall fatigue S - N curve, the stress amplitude corresponding to a fatigue life of 2 million cycles for the welded steel bar was approximately 128.72 MPa. Compared with the base metal, the stress amplitude decreased by 45.75%. The stress amplitude under ultra - high cyclic loading was predicted. The coupling relationship of stress-amplitude stress-ratio fatigue-cycle was fitted and analyzed, relevant equations were derived, and a safety line for the values of stress amplitude and stress ratio was determined.

ARTICLE HISTORY

Received: 26 February 2025
Revised: 26 June 2025
Accepted: 26 June 2025

KEYWORDS

Cross-welded steel bars;
Fatigue test;
S-N curve;
Stress ratio;
Fatigue performance

Copyright © 2026 by The Hong Kong Institute of Steel Construction. All rights reserved.

1. Introduction

With the rapid expansion of the high - speed railway network in China, the construction technology for high - speed railways has also advanced significantly [1-2]. In the simply - supported box girders of high - speed railways, a large number of steel bars are arranged to form a steel fabric. Traditionally, the steel fabric is fabricated manually by workers, which leads to low efficiency, slow construction progress, and high costs. With the advancement of intelligent construction technology in high - speed railway bridge construction[3], automatic spot welding construction has been adopted to substitute the manual binding of steel bars in the construction of steel fabric. This not only significantly enhances construction efficiency, cuts down labor costs, but also speeds up the progress of bridge construction. However, fatigue issues of welded steel bars emerge subsequently[4-5]. Traditional manual construction methods do not damage the steel bars, but automatic spot welding can cause localized damage to the steel bar. When high - speed trains frequently pass over the bridges, the dynamic loads generated may lead to fatigue damage of the steel bars, thereby affecting the operational safety of the entire bridge. Therefore, it is essential to investigate the fatigue performance of welded steel bars[6-8].

For the fatigue performance of welded steel, scholars both at home and abroad have conducted relevant research[9-12]. For welded steel bars, Wang et al. [13] carried out fatigue tests on HRB400 electric arc - welded steel bars. The test results indicated that the fatigue strength decreased slightly as the stress ratio and the diameter of the steel bars increased. The design p - S - N curve of the electric arc - welded steel bars was obtained through fitting. Sheng et al. [14] performed low - frequency and high - frequency fatigue tests on steel bars of different specifications and diameters to derive the S - N curves. Zheng et al. [15] conducted experimental research and analysis on the fatigue strength of flash - butt welding specimens made of HRB500 high strength steel. The fatigue strengths of the base metal and the weldment were determined using the S - N curve and the lifting method. In addition, China's codes also contain relevant provisions regarding the fatigue performance of welded steel bars. In the "Code for Design of Concrete Structures of Railway Bridges and Culverts (TB10092 - 2017)" [16], the fatigue strengths of the base metal, flash - butt welding, electric arc welding, and other welding forms are specified. The allowable fatigue stress amplitudes of the base metal, flash - butt welding, and electric arc welding are 145 MPa, 130 MPa, and 60 MPa respectively. In the "Code for Design of Concrete Structures (GB 50010 - 2010)" [17], the fatigue stress amplitudes of HRB400 steel bars with different stress ratios range from 31 MPa to 175 MPa.

The objects of the above research and codes are only for the base metal or the welded joint of two steel bars in the same straight line. However, in the steel fabric of the simply - supported box girder of the high - speed railway, the steel bar connections are cross - welded spot connections. For this type of cross - welded spot connection, after the steel bars are cross - welded, they remain continuous through - length bars. Only at the welded spot positions of the steel bars, the base metal suffers certain damage. The cross - welded spot connection differs from the aforementioned flash - butt welding steel bars where the two steel bars form a welded joint in the same straight line. For the cross - welded steel bars, Schwarzkopf [18] verified the fatigue limit state and established a fatigue limit state verification method based on the Palmgren - Miner rule. Gu et al. [19, 20] investigated the fatigue performance of welded steel fabrics made of cold - rolled ribbed steel bars (CRB550), hot - rolled ribbed steel bars (HRB400), and high ductility cold - rolled ribbed steel bars (CRB600H), and presented S - N curve equations. Li et al. [21] conducted high cycle fatigue tests on base metal specimens and specimens with welded joints at different stress levels. The fatigue performance of both was analyzed. The S - N curves and p - S - N curves were obtained, and fatigue reliability analysis was performed. As can be seen, although the fatigue performance of cross - welded steel bars has been studied both domestically and internationally, the relevant literature is still very limited. Currently, for the fatigue performance of cross - welded spot steel bars in high - speed railway box girders, there is no relevant code in China. Only in the "Technical Specification for Concrete Structures with Welded Steel Fabric (JGJ114 - 2014)" [22], Article 3.1.7 stipulates that when welded steel fabrics made of CRB550, CRB600H, and HRB400 steel bars are used for plate flexural members, fatigue performance needs to be checked. When the maximum stress of the steel bar does not exceed 300 MPa, the limit value of the fatigue stress amplitude for 2 million cycles can be taken as 100 MPa. It is evident that the codes are very rough and not suitable for the fatigue of cross - welded steel bars in high - speed railway box girders. The research on the fatigue performance of cross - welded steel bars in high - speed railway box girders is still in its initial stage. It is necessary to conduct further in - depth studies on the fatigue performance of cross - welded steel bars.

In this paper, the fatigue performance of cross - welded steel bars was investigated. Based on the test results, the fatigue S - N curve of the cross - welded steel bars was derived through fitting. The research findings offer theoretical support for the operational safety of high - speed railways and serve as a reference for the future formulation of relevant codes. This paper is divided into six parts. Firstly, the “Introduction” summarizes the current research status of the fatigue performance of welded steel bars, with a primary focus on those used in China. Secondly, the “Test Overview” describes the specimens of welded steel bars, including specimen fabrication and testing methods. Thirdly, the “Test results and analysis” mainly focuses on analyzing the test results and the failure of the specimens. Fourthly, the “Fatigue S - N Curves” section theoretically analyzes the fatigue test results and fits the fatigue S - N curves under different working conditions. Fifthly, the “Further study on fatigue performance” mainly explores the fatigue performance of cross - welded steel bars under ultra - high cycle loads and the influence of coupling factors on fatigue life. Finally, the “Conclusion” summarizes the findings of the research in this paper.

2. Test overview

2.1. Specimen design

Referring to relevant literature[19,20], the specimen was designed as a cross - connection of two steel bars. One was a 300 mm long steel bar, and the other was a 40 mm long steel bar, as shown in Fig. 1. According to the diameter of the steel bars, the specimens were divided into five groups, namely M1 - M5. Among them, in the M4 and M5 groups, a 19 mm × 0.9 mm steel strip was welded onto the steel bars, as shown in Table 1. In addition, to compare the effect of welding on the fatigue performance of steel bars, fatigue tests were also conducted on the base metal specimens. Each base metal specimen was 300 mm long and 12 mm in diameter, and there were 3 base metal specimens in total. All specimens were made of HRB400 steel bars.

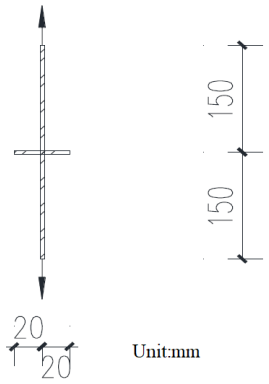

Fig. 1 Detailed specimen dimension

Table 1
Specimen groups

Group	Direction	Diameter /mm
M1	Longitudinal	12
	Transverse	16
M2	Longitudinal	12
	Transverse	12
M3	Longitudinal	12
	Transverse	18
M4	Longitudinal	18
	Transverse	19×0.9 steel strip
M5	Longitudinal	12
	Transverse	19×0.9 steel strip
Base metal	Longitudinal	12

2.2. Fatigue loading scheme

Fatigue tests were conducted under different stress ratios and stress amplitudes. For each of the specimen groups from M1 to M5, there were many working conditions, and two specimens were used for each working condition, resulting in a total of 126 specimens. The stress ratio had three levels: 0.1, 0.2, and 0.4. The stress amplitude was set at intervals of 100 MPa, with a maximum stress of 400 MPa to cover the stress range of the HRB400 steel bars. The working conditions of the fatigue tests are presented in Table 2.

Based on the loading mode of fatigue load, fatigue tests can be classified into constant amplitude loading and variable amplitude loading. In this test, constant amplitude loading was adopted, as shown in Fig. 2. The fatigue test was carried out at room temperature. The steel bars were subjected to tension - tension loading with a sinusoidal load at a frequency of 20 Hz. According to Chinese codes [22, 23], the test would be terminated if the specimen had not fractured after reaching 2 million cycles. Three specimens were prepared for the fatigue test of the base metal. The maximum stresses were set at 400 MPa, 350 MPa, and 300 MPa respectively, and the stress ratio was set at 0.2, as shown in Table 2. The fatigue loading mode of the base metal was the same as that of the welded specimens.

Table 2
Fatigue test working conditions of M1~M5 and base metal

Stress ratio	Maximum stress /MPa	Minimum stress /MPa	Stress amplitude /MPa	Number of specimens	Note
0.1	400	40	360	2	M1~M5
	300	30	270	2	
	200	20	180	2	
	100	10	90	2	
0.2	400	80	320	2	
	300	60	240	2	
	200	40	160	2	
	100	20	80	2	
0.4	400	160	240	2	
	300	120	180	2	
	200	80	120	2	
	100	40	60	2	
0.2	400	80	320	1	Base metal
	350	70	280	1	
	300	60	240	1	

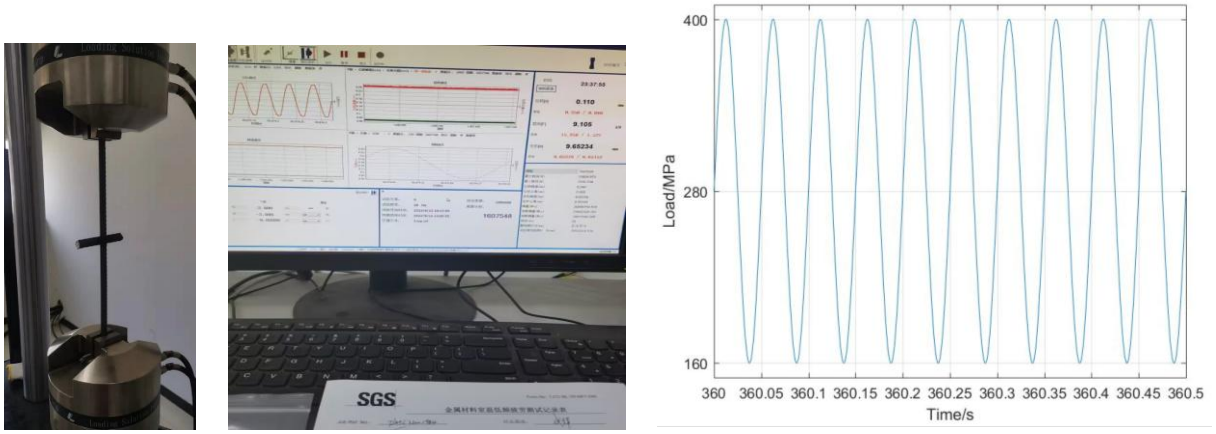

(a) Fatigue testing (b) Data acquisition (c) Load history diagram of fatigue test

Fig. 2 Fatigue test

3. Test results and analysis

3.1. Static test

To assess the impact of welding on the static mechanical properties of steel bars, three cross-welded specimens were randomly chosen for the static tensile test prior to the fatigue test. The yield strength and ultimate tensile

strength values of the specimens are presented in Table 3. As shown in Table 3, the static strength of the specimens did not decrease. This indicates that the static properties of the steel bars were not significantly affected by welding. The possibility that the static strength of the steel bars could decrease due to welding factors, which could in turn affect the fatigue performance, was ruled out.

Table 3
Static test results

	M1	M2	M3
Yield strength /MPa	400	445	435
Ultimate strength /MPa	635	675	635

3.2. Specimen failure diagram

The failure diagrams of the static and fatigue tests of the specimens are shown in Fig. 3. As shown in Fig. 3(a), when the specimen was subjected to static tension, the failure occurred at the non-welded position. The specimen exhibited an obvious necking fracture, and the steel bar yielded, which was a typical ductile failure. As shown in Fig. 3(b), when the specimen was subjected to a fatigue load, the failure occurred at the cross-welded position. Part of the cross-section was smooth, while the other part was relatively rough. A corrugated fatigue fracture could be observed. The reason for this lies in the fatigue damage process. Firstly, there were welding defects at the welded position of the specimen. Welding would cause local heating of the steel bar, and the uneven temperature field would lead to local plastic deformation of the steel bar. After welding, residual stress and stress concentration were generated in the steel bar. The area with residual stress and stress concentration near the welding point of the steel bar was a pre-existing defect. It was easy for this area to form the initial source of fatigue. Under the action of the fatigue load, fatigue micro-cracks originated from the fatigue source and propagated. As the number of repeated loads increased, the crack propagation zone was gradually formed. The interface within the crack propagation zone was continuously rubbed and squeezed under the cyclic load, thus forming a smooth section area. When the crack propagation zone had propagated to the critical size, the remaining area of the steel bar was insufficient to bear the external fatigue load, and the specimen suddenly fractured. Unlike the ductile failure of the specimen under static tension, fatigue failure was a sudden brittle failure, which posed a hazard.

(a) Static failure of specimens

(b) Fatigue failure of specimens

Fig. 3 Comparison of static and fatigue failure

Table 4
Fatigue test results of the M1 group

Stress ratio	Specimen number	Number of cycles /×10^4	Fracture position	Specimen number	Number of cycles	Fracture position
0.1	M1-0.1-400-1	9.4188	Non-welded area	M1-0.1-400-2	10.2685	Welding position
	M1-0.1-300-1	35.557	Welding position	M1-0.1-300-2	44.9155	Welding position
	M1-0.1-200-1	200	No fracture	M1-0.1-200-2	200	No fracture
	M1-0.1-100-1	200	No fracture	M1-0.1-100-2	200	No fracture
0.2	M1-0.2-400-1	7.3595	Welding position	M1-0.2-400-2	9.3068	Welding position
	M1-0.2-300-1	43.3597	Welding position	M1-0.2-300-2	41.6827	Welding position
	M1-0.2-200-1	200	No fracture	M1-0.2-200-2	200	No fracture
	M1-0.2-100-1	200	No fracture	M1-0.2-100-2	200	No fracture
0.4	M1-0.4-400-1	19.6338	Welding position	M1-0.4-400-2	18.9725	Welding position
	M1-0.4-300-1	176.6307	Welding position	M1-0.4-300-2	62.464	Welding position
	M1-0.4-200-1	200	No fracture	M1-0.4-200-2	200	No fracture
	M1-0.4-100-1	200	No fracture	M1-0.4-100-2	200	No fracture

Note: M1 represents the grouping number, 0.1 represents the test stress ratio, 400 represents the maximum stress, and 1 indicates that it is the No.1 specimen under the working condition. No fracture indicates that the specimen is not damaged by fatigue after 2 million cycles and the test is terminated.

3.3. Fatigue test results

Based on the aforementioned fatigue test scheme, the fatigue test was carried out, and the test results of the M1 group are presented in Table 4. The results of the other groups are similar and will not be listed here. The test data points are plotted on the double - logarithmic coordinate system, as shown in Fig. 6 below. For the test working condition with a maximum stress of 400 MPa, it is evident from the test results that fatigue damage occurred in all specimen groups. For the test working condition with a maximum stress of 300 MPa, only one specimen in the M3 group with a stress ratio of 0.1 reached 2 million cycles without fatigue failure, while the rest of the specimens experienced fatigue failure. For the test working condition with a maximum stress of 200 MPa, most of the specimens did not undergo fatigue failure after 2 million cycles. For the test working conditions with a maximum stress below 200 MPa, no fatigue failure occurred in any of the specimens. At a stress ratio of 0.1 and a maximum stress of 200 MPa, the stress amplitude was 180 MPa. Accordingly, it can be predicted that the stress amplitude for 2 million cycles at a stress ratio of 0.1 should be greater than 180 MPa. Similarly, it can be predicted that the stress amplitudes for 2 million cycles at stress ratios of 0.2 and 0.4 should be higher than 160 MPa and 120 MPa, respectively.

4. Fatigue S-N curves

4.1. Fatigue S-N curve fitting method

There are several fitting models for the fatigue S - N curve of steel bars. Currently, the mathematical expressions of the fatigue S - N curve are mainly the exponential function, power function, and three - parameter power function [24-25], which correspond to the single - logarithm linear model, double - logarithm linear model, and double - logarithm three - parameter power function model, respectively. Additionally, based on the double - logarithmic linear model, a double - logarithmic polyline model is derived by setting an inflection point at a certain location. Considering the advantages and disadvantages of each model and referring to the European standard "Design of Steel Structures - Part 1 - 9: Fatigue EN 1993 - 19:2005" [26], the fatigue S - N curve in this study is fitted using the double - logarithmic polyline model, with a fatigue life of 2 million cycles as the inflection point. The fatigue S - N curve of the double - logarithmic polyline model consists of two straight - line segments. The first segment is represented by a line segment with a steeper slope, corresponding to a fatigue life of less than 2 million cycles. It is fitted using the least - squares method based on the power - function curve equation.

$$NS^m = \mathrm{C} \tag{1}$$

In the above equation, m and C are two constants determined experimentally. In this paper, the relationship between the number of fatigue cycles and the stress amplitude is investigated. The stress amplitude is defined as $S = \Delta\sigma = \sigma_{max} - \sigma_{min}$. Taking the logarithm for both sides of Equation (1), Equation (2) is derived as follows.

$$lgN = \mathrm{b} + \mathrm{m}lg\Delta\sigma \tag{2}$$

From equation (2), it is evident that the exponential function expression is equivalent to the linear relationship between $lg\Delta\sigma$ and lgN in semi - logarithmic coordinates. Therefore, the model obtained by this method is generally referred to as a linear model, which represents the nonlinear relationship in a linear logarithmic equation.

The second segment is represented by a line segment with a slope m=m+2, corresponding to a fatigue life of more than 2 million cycles. The reason for setting the slope m=m+2 is that the stress amplitude at a low-stress level is not simply linearly related to that at a high-stress level, A commonly used approach is to adopt m=m+2 as the slope to reflect the characteristics of fatigue life at low-stress level[27].

Considering the survival rate (i.e., reliability), the fatigue S-N curve is corrected. A common method is to add the deviation obtained from test point statistics to equation (2) [28], as shown in Equation (3). In the Equation (3), $c = \alpha m_N\sqrt{1-\theta^2}$, where m_N is the logarithm mean squared deviation of the cycle number, and θ is the correlation coefficient. When $\alpha = 2$, the survival rate is 97.7%.

$$lgN = \mathrm{b} + \mathrm{m}lg\Delta\sigma + \mathrm{c} \tag{3}$$

4.2. Fatigue S-N curve of base metal

The fatigue test results of the base metal are presented in Fig. 4. As can be seen, when the stress amplitude decreased from 320 MPa to 280 MPa, the fatigue life increased by 253,300 cycles, a 2.53 - fold increase. When the stress amplitude decreased from 280 MPa to 240 MPa, the fatigue life increased by 1,458,500 cycles, a 4.48 - fold increase. It is evident that the stress amplitude has a significant impact on the fatigue life, and the number of fatigue cycles decreases nonlinearly as the stress amplitude increases. According to the test results, the rate of decrease in fatigue life in the stress amplitude range of 240 MPa to 280 MPa is higher than that in the range of 280 MPa to 320 MPa, indicating a higher sensitivity of fatigue life to low - stress amplitudes.

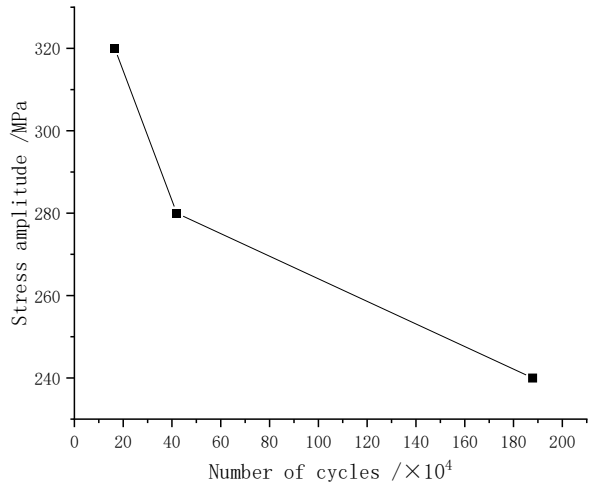

Fig. 4 Fatigue test results of base metal

The fatigue S - N curves of the base metal were derived through fitting based on the fatigue test results, as presented in Table 5. These curves were plotted out in a double - logarithmic coordinate system, as shown in Fig. 5. The stress amplitude corresponding to a fatigue life of 2 million cycles calculated by the fitting curve was approximately 236.49 MPa. After correcting the fitting results according to a survival rate of 97.7%, the fatigue stress amplitude for 2 million cycles was approximately 230.16 MPa. Notably, this value was higher than the stress amplitude of 156 MPa for HRB400 steel bars specified in the "Code for Design of Concrete Structures"[17] under the condition of a stress ratio of 0.2.

Table 5
Fatigue S-N curve equation for base metal

Fatigue S-N curve	R-squared of fitting	Stress amplitude for 2 million cycles /MPa		
		Test value	Correction value	Decrease rate
lg*N*=26.40113-8.46742lg*Δσ* (*N*≤2000000) lg*N*=31.14876-10.46742lg*Δσ* (*N*≥2000000)	0.99	236.49	230.16	2.75%

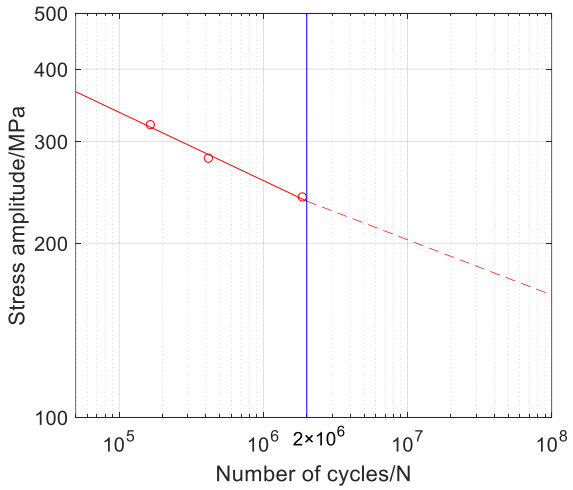

Fig. 5 Fatigue S-N curve of base metal

4.3. Fatigue S-N curve analysis under each working condition

Based on the test results, the fatigue S - N curves of Groups M1 - M5 under different stress ratios were fitted, as presented in Table 6. The calculated stress amplitude for 2 million cycles ranges from a minimum of 91.87 MPa in the M4 group under the stress ratio of 0.4 to a maximum of 194.03 MPa in the M1 group under the stress ratio of 0.1, with an average stress amplitude of 147.61 MPa. After correcting the fitting results according to a survival rate of 97.7%, the modified stress amplitudes were obtained. The stress amplitudes of each group decreased to varying degrees, ranging from approximately 3.36% to 24.87%, with an average decrease of 12.09%. The modified minimum stress amplitude was 81.19 MPa, the maximum was 186.10 MPa, and the average was 130.36 MPa.

Comparing with the conclusions drawn from the analysis of test results in Section 3.3 above, where the stress amplitudes for 2 million cycles at the three stress ratios should be higher than 180 MPa, 160 MPa, and 120 MPa, the stress amplitudes obtained from the fatigue S - N curves were lower. This indicates that the stress amplitudes obtained by the linear fitting method are relatively conservative.

From the fitted curve, it can be clearly seen that when the stress amplitude was constant, the fatigue life decreased with the increase of the stress ratio. This law was particularly evident in M1 to M4. For M5, the fatigue S - N curve corresponding to a stress ratio R=0.4 was higher. Moreover, the fatigue S-N curves fitted for the stress ratios R=0.2 and R=0.1 showed relatively higher coincidence compared with the stress ratio R=0.4, indicating that as the stress ratio increased, the sensitivity of fatigue life to the stress ratio gradually increased.

Table 6
Fatigue S-N curves for each group with different stress ratios

Groups	Stress ratios	Fatigue S-N curve	R-squared of fitting	Strss amplitude for 2 million cycles /MPa		
				Test value	Correction value	Decrease rate
M1	0.1	$\lg N=17.45131-4.87366\lg\Delta\sigma$ ($N\leq2\times10^6$) $\lg N=22.02704-6.87366\lg\Delta\sigma$ ($N\geq2\times10^6$)	0.984	194.03	186.10	4.09%
	0.2	$\lg N=19.16802-5.68836\lg\Delta\sigma$ ($N\leq2\times10^6$) $\lg N=23.69199-7.68836\lg\Delta\sigma$ ($N\geq2\times10^6$)	0.990	182.80	176.66	3.36%
	0.4	$\lg N=19.30300-5.88915\lg\Delta\sigma$ ($N\leq2\times10^6$) $\lg N=23.71856-7.88915\lg\Delta\sigma$ ($N\geq2\times10^6$)	0.841	161.36	139.69	13.43%
M2	0.1	$\lg N=13.92056-3.48984\lg\Delta\sigma$ ($N\leq2\times10^6$) $\lg N=18.28725-5.48984\lg\Delta\sigma$ ($N\geq2\times10^6$)	0.574	152.53	114.59	24.87%
	0.2	$\lg N=17.26281-4.88849\lg\Delta\sigma$ ($N\leq2\times10^6$) $\lg N=21.74754-6.88849\lg\Delta\sigma$ ($N\geq2\times10^6$)	0.799	174.73	147.88	15.37%
	0.4	$\lg N=15.23831-4.17604\lg\Delta\sigma$ ($N\leq2\times10^6$) $\lg N=19.51858-6.17604\lg\Delta\sigma$ ($N\geq2\times10^6$)	0.766	138.08	114.91	16.78%
M3	0.1	$\lg N=15.50731-4.10088\lg\Delta\sigma$ ($N\leq2\times10^6$) $\lg N=19.99721-6.10088\lg\Delta\sigma$ ($N\geq2\times10^6$)	0.967	175.77	165.28	5.97%
	0.2	$\lg N=12.71205-3.02412\lg\Delta\sigma$ ($N\leq2\times10^6$) $\lg N=16.95197-5.02412\lg\Delta\sigma$ ($N\geq2\times10^6$)	0.813	131.81	112.39	14.73%
	0.4	$\lg N=16.70012-4.80759\lg\Delta\sigma$ ($N\leq2\times10^6$) $\lg N=21.02623-6.80759\lg\Delta\sigma$ ($N\geq2\times10^6$)	0.998	145.56	143.21	1.62%
M4	0.1	$\lg N=13.29931-3.29484\lg\Delta\sigma$ ($N\leq2\times10^6$) $\lg N=17.54733-5.29484\lg\Delta\sigma$ ($N\geq2\times10^6$)	0.978	133.05	121.23	8.89%
	0.2	$\lg N=13.6621-3.44057\lg\Delta\sigma$ ($N\leq2\times10^6$) $\lg N=17.94108-5.44057\lg\Delta\sigma$ ($N\geq2\times10^6$)	0.950	137.88	119.51	13.32%
	0.4	$\lg N=10.24624-2.00962\lg\Delta\sigma$ ($N\leq2\times10^6$) $\lg N=14.17256-4.00962\lg\Delta\sigma$ ($N\geq2\times10^6$)	0.998	91.87	81.19	11.62%
M5	0.1	$\lg N=13.32842-3.29892\lg\Delta\sigma$ ($N\leq2\times10^6$) $\lg N=17.58884-5.29892\lg\Delta\sigma$ ($N\geq2\times10^6$)	0.885	134.96	119.74	11.28%
	0.2	$\lg N=14.36774-3.77073\lg\Delta\sigma$ ($N\leq2\times10^6$) $\lg N=18.64633-5.77073\lg\Delta\sigma$ ($N\geq2\times10^6$)	0.899	137.82	123.29	10.54%
	0.4	$\lg N=16.66334-4.72691\lg\Delta\sigma$ ($N\leq2\times10^6$) $\lg N=21.04773-6.72691\lg\Delta\sigma$ ($N\geq2\times10^6$)	0.962	155.67	145.67	6.42%

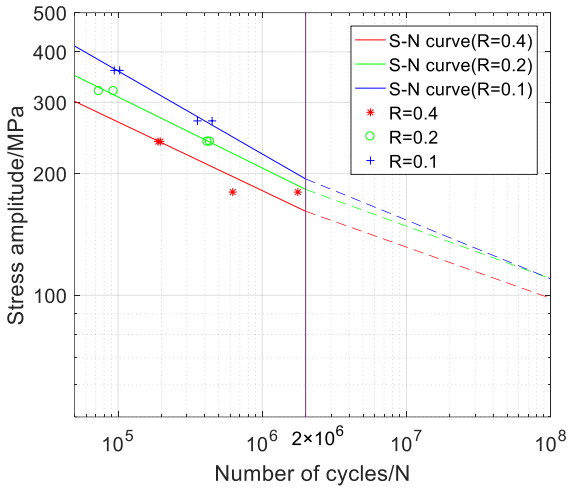

(a) Fatigue S-N curves for M1

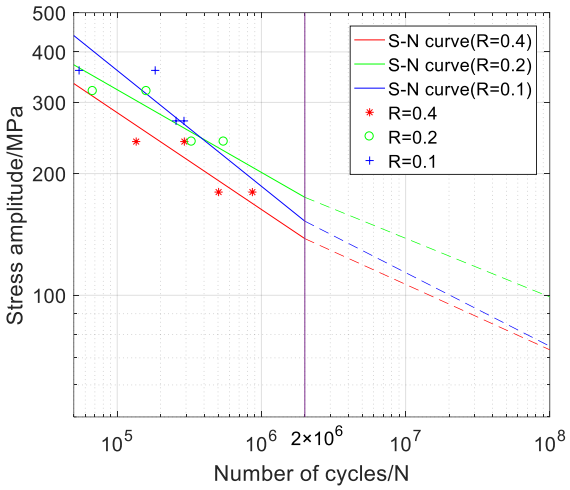

(b) Fatigue S-N curves for M2

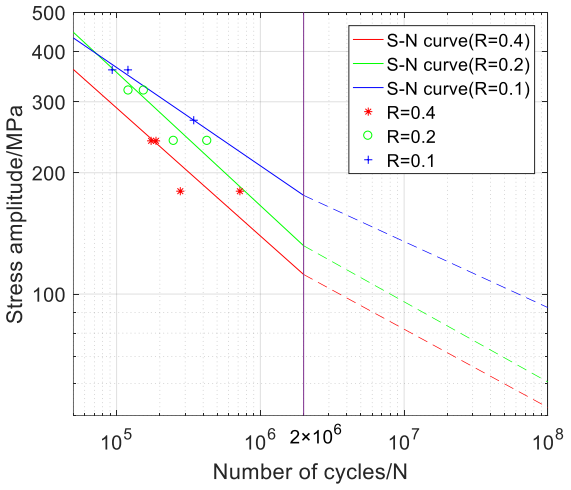

(c) Fatigue S-N curves for M3

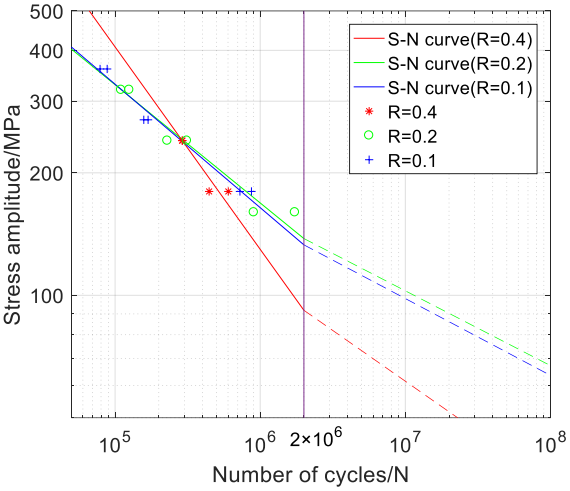

(d) Fatigue S-N curves for M4

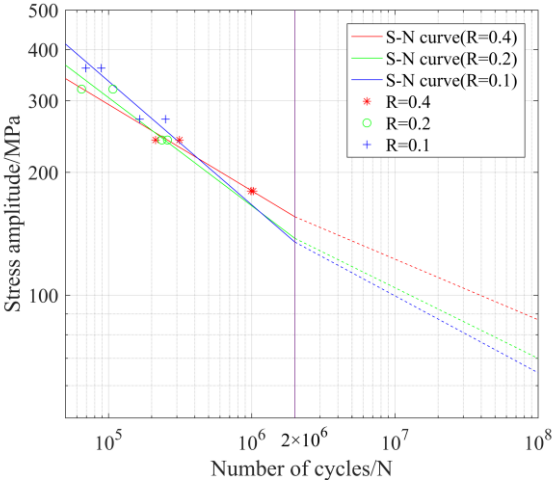

(e) Fatigue S-N curves for M5

Fig. 6 Fatigue S-N curves for each group with different stress ratios

The stress amplitudes of the five groups under different stress ratios were analyzed. Based on the stress amplitude and stress ratio for 2 million cycles in Table 6, the relationship curve was fitted and presented in Table 7. Sheng et al [14] combined his test results with the suggested values of stress amplitude and stress ratios in the "Code for the Design of Concrete Structures" [17] to fit the relationship curve between stress amplitude and stress ratio. To facilitate comparison, the curves provided by Sheng et al. were equivalently transformed. Similarly, corresponding equations were fitted according to the values specified in the code. The comparison among the test results of this paper, the stress amplitude stress ratio curves from the literature [14], and the code [17] is shown in Fig. 7. It can be observed that the smaller the stress ratio, the smaller the slope of the curve, and the sensitivity of the fatigue stress amplitude to the stress ratio gradually decreased as the stress ratio increased.

4.4. Analysis of total fatigue S-N curve

In Section 4.3 above, the fatigue S - N curve analysis was conducted for each working condition of Groups M1 - M5. To gain an overall understanding of the fatigue performance of cross - welded steel bars, all test data under various working conditions were integrated to fit the fatigue S - N curve, as presented in Table 8. The fatigue S - N curves of the cross - welded steel bars as a whole and the base metal are shown in Fig. 8. It is evident that welding has a significant impact on the fatigue performance of steel bars, notably reducing their fatigue life. As the stress amplitude increases, the fatigue life of the welded steel bars decreases rapidly, much faster than that of the base metal. The stress amplitude of the cross - welded steel bars for 2 million cycles is 128.72 MPa, while that of the base metal is 236.49 MPa. The stress amplitude of the cross - welded steel bars is 45.75% lower than that of the base metal.

Based on a survival rate of 97.7%, the fitting results were corrected. After correction, the stress amplitude of the welded steel bars for 2 million cycles was 100.49 MPa, while that of the base metal was approximately 230.16 MPa. The stress amplitude of the welded steel bars was 56.34% lower than that of the base metal. In literature [20], the reported stress amplitude was 156.64 MPa. In the European code [29], the specified stress amplitude was about 100.04 MPa, and in the German code [30], it was around 99.17 MPa. These results are summarized in Table 9. Evidently, the modified test results were lower than those reported in literature [20] and close to the values specified in the codes [29-30].

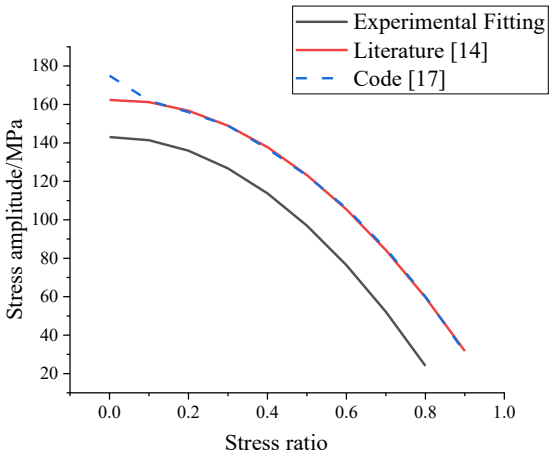

Fig. 7 Stress amplitude stress ratio relationship curve

Table 7
Stress amplitude stress ratio relationship equation

Item	Equation	Note
Experimental Fitting	$\Delta\sigma = -188.82\rho^2 + 2.25\rho + 143.049$	In the equation: ρ indicates the stress ratio, and $\Delta\sigma$ indicates the stress amplitude.
Literature [14]	$\Delta\sigma = -167.44\rho^2 + 5.6\rho + 162.32$	
Code [17]	$\Delta\sigma = -138.63\rho^2 - 27.2\rho + 170.16$	

Table 8
Fatigue S-N curve for total cross-welded steel bars

Fatigue S-N curve equation	R-squared of fitting	Stress amplitude for 2 million cycles and decreasing rate			
		Test value /MPa	Decreasing rate/MPa	Correction value/MPa	Decreasing rate/%
lg$N$=12.80034-3.08075lg$\Delta\sigma$ (N≤2×10⁶) lg$N$=17.01964-5.08075lg$\Delta\sigma$ (N≥2×10⁶)	0.796	128.72	45.75	100.49	56.34

Table 9
Summary and comparison of stress amplitude

Item	Test	Test correction	Base metal	Literature [20]	Code[29]	Code[30]
Stress amplitude /MPa	128.72	100.49	230.16	156.64	100.04	99.17

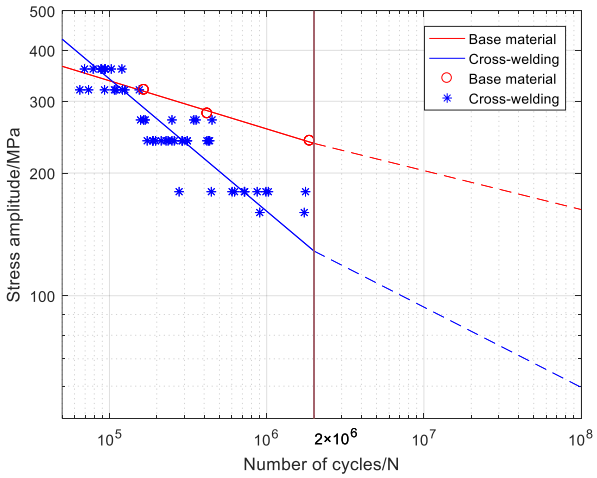

Fig. 8 Comparison of fatigue S-N curves between welded steel bar and base metal

5. Further study on fatigue performance

5.1. Ultra-high cycle stress amplitude

The existing codes use 2 million fatigue cycles as an important indicator to measure the fatigue life of steel bars in building structures. However, high - speed railways operate at high speeds and with high frequency. In an actual simply - supported box girder, the number of fatigue cycles of steel bars may far exceed 2 million. Currently, China's high - speed railway codes do not explicitly specify the fatigue life of steel bars. In this paper, it is assumed that a high - speed train runs on a high - speed railway line every 5 minutes. According to the design service life of 100 years, the number of fatigue cycles of steel bars will exceed 10 million. The literature [20, 31-32] has indicated that the number of high - speed train operations can reach hundreds of millions within the design service life. Evidently, using 2 million cycles as an indicator of fatigue life does not meet the actual needs of high - speed railway operation. Therefore, the stress amplitude under ultra - high cyclic loads should be studied.

The stress amplitudes from this test and different literatures under different fatigue cycle numbers under ultra - high cyclic loads are listed in Table 10. The stress amplitude under ultra - high cyclic loads is predicted from the fatigue S - N curve obtained in Section 4. For comparison, based on relevant literatures, the inflection point of the fatigue curve was set at 10 million cycles. When the number of fatigue cycles exceeded 10 million, the stress amplitude of the steel bar dropped below 80 MPa. Considering the survival rate, the corrected stress amplitude was only 59.60 MPa, which was 42.46% lower than the results reported in literature [19], but close to the results specified in the codes [29-30]. It can also be observed from Fig. 9 that the test results in this paper lie between the results reported in literatures [19- 20] and those specified in the codes [29-30]. The modified curve shows a high degree of consistency with the fatigue S - N curves given in the codes [29-30].

Table 10
Stress amplitude at ultra-high cycle load

No.	Source	Fatigue S-N curve	Stress amplitude for different fatigue cycles /MPa						
			1×10^6	2×10^6	4×10^6	6×10^6	8×10^6	10^7	10^8
1	Test	$\lg N=12.80034-3.08075\lg\Delta\sigma$ ($N<10^7$) $\lg N=17.01964-5.08075\lg\Delta\sigma$ ($N\geq10^7$)	161.20	128.72	102.79	90.11	82.08	76.34	48.52
2	Test correction	$\lg N=12.80034-3.08075\lg\Delta\sigma$ ($N<10^7$) $\lg N=16.56588-5.08075\lg\Delta\sigma$ ($N\geq10^7$)	125.85	100.49	80.25	70.35	64.08	59.60	37.88
3	Literature [20]	$\lg N=14.7811-3.8639\lg\Delta\sigma$ ($N<10^7$) $\lg N=18.8081-5.8639\lg\Delta\sigma$ ($N\geq10^7$)	187.33	156.56	130.85	117.82	109.36	103.23	69.70
4	Literature [20]	$\lg N=19.5581-5.9792\lg\Delta\sigma$ ($N<10^7$) $\lg N=23.7563-7.9792\lg\Delta\sigma$ ($N\geq10^7$)	185.16	164.89	146.84	137.21	130.77	125.98	94.40
5	Literature [19]	$\lg N=12.3214-3.0\lg\Delta\sigma$ ($N<10^7$) $\lg N=15.8690-5.0\lg\Delta\sigma$ ($N\geq10^7$)	127.98	101.58	80.62	70.43	63.99	59.40	37.48
6	Code[29]	$\lg N=12.3016-3.0\lg\Delta\sigma$ ($N<10^7$) $\lg N=15.8360-5.0\lg\Delta\sigma$ ($N\geq10^7$)	126.05	100.04	79.40	69.37	63.02	58.51	36.91
7	Code [30]	$\lg N=12.2902-3.0\lg\Delta\sigma$ ($N<10^7$) $\lg N=15.8170-5.0\lg\Delta\sigma$ ($N\geq10^7$)	124.95	99.17	78.71	68.76	62.47	58.00	36.59

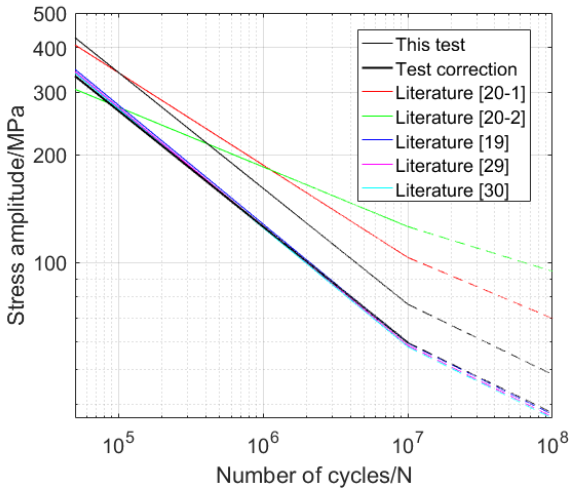

Fig. 9 Comparison of the fatigue S-N curve for cross-welded steel bars

5.2. Analysis of multi-factor coupling influence on fatigue life

The effects of stress amplitude and stress ratio on fatigue life were derived from the test results and fitting fatigue S-N curves. In the three-dimensional coordinate system, taking the stress - amplitude, stress - ratio, and fatigue - cycle as coordinate parameters, the curved surfaces of three influencing factors were fitted. The curved surfaces equation is listed in Equation (4), the fitting R variance is 0.7127, and the curved surface of stress - amplitude stress - ratio fatigue - cycle is shown in Fig. 10 (a). From Fig. 10 (a), the characteristics of the three factors can be observed. When the stress - amplitude is smaller, the fatigue - cycle is higher and the stress - ratio is larger, the curvature of the surface is larger, indicating that in the low-stress amplitude region with high fatigue life, the fatigue - cycle is more sensitive to the stress - amplitude. The greater the stress ratio is, the stronger the sensitivity is.

The intersection line between a plane representing 2 million fatigue cycles and the surface was determined. This intersection line was projected onto the stress - amplitude stress - ratio plane, and the relationship curve between stress - amplitude and stress - ratio was obtained, as shown in Fig. 10 (b). The curve divides the coordinate system into two regions. The values of stress - amplitude and stress - ratio in the region below the curve meet the requirement of 2 million cycles. Under the corresponding working conditions of stress - amplitude and stress - ratio in this region, the fatigue performance of cross - welded steel bars can be ensured.

A comparison of the stress - amplitude stress - ratio curves between Fitting Method 1 in Section 4.3 (Fig. 7) and Fitting Method 2 (Fig. 10) is presented in Fig. 11. As can be observed from Fig.11, there was little difference between the two methods in the stress ratio range of 0 to 0.4, and the error was within 10%. However, the difference between the two methods gradually increased when the stress ratio exceeded 0.4.

Based on the fatigue S - N curve obtained through the linear fitting method in Table 6, the fatigue lives under different working conditions were obtained and compared with the experimental results. The average error was 31.12%. When the fatigue lives obtained by the three - dimensional fitting method were compared with the experimental results, the average error was 18.54%. The three - dimensional fitting method outperforms the linear fitting method in the stress ratio range of 0 to 0.4. In actual engineering, fatigue cyclic loads with a stress ratio greater than 0.4 are rare, and the available data is insufficient. Accurately predicting the stress - amplitude stress - ratio relationship may require more test data for support.

$$f(x,y)=p_{00}+p_{10}x+p_{01}y+p_{20}x^2+p_{11}xy+p_{30}x^3+p_{21}x^2y \quad (4)$$

Where x is the stress amplitude, y is the stress ratio, and the coefficients are taken as shown in Table 11.

Table 11
Curvilinear equation coefficients

Parameter	p_{00}	p_{10}	p_{01}	p_{20}	p_{11}	p_{30}	p_{21}
Coefficients Value	1.218×10^7	-1.231×10^5	4.951×10^6	422.3	4.472×10^4	- 0.4767	- 106.4

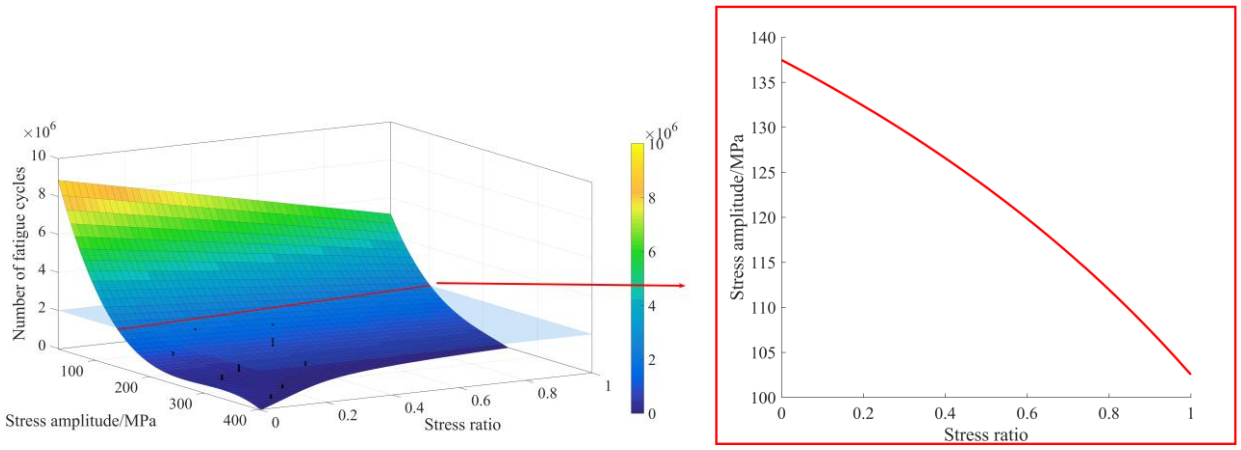

(a) Surface of stress-amplitude stress- ratio fatigue-cycle (b) Line for stress-amplitude stress- ratio

Fig. 10 The curved surface of stress-amplitude stress- ratio fatigue-cycle

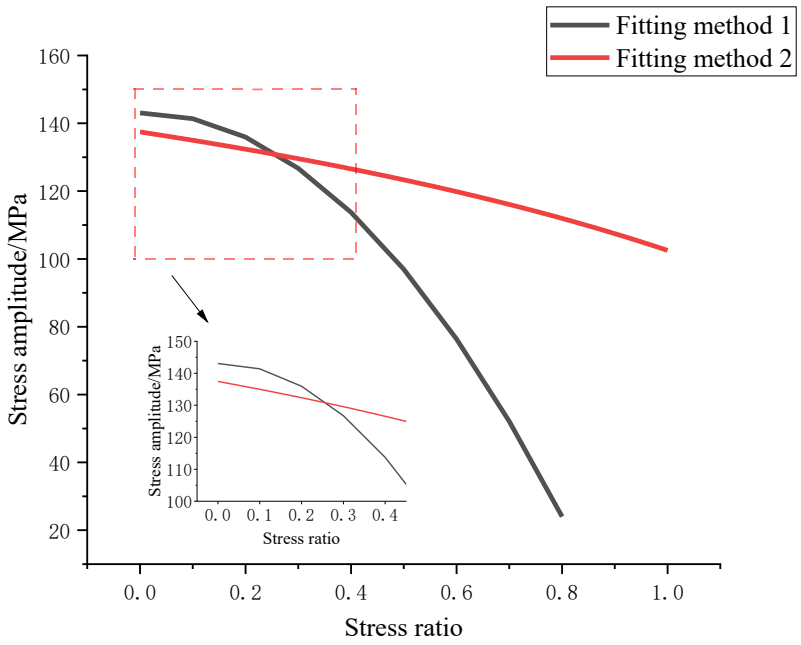

Fig. 11 Comparison of stress-amplitude stress-ratio curve

6. Conclusions

For the fatigue performance of steel bars in the simply - supported box girders of high - speed railways, this paper conducts experimental research and theoretical analysis on cross - welded steel bars and the base metal. The main conclusions of this study are as follows.

(1) Welding does not have a significant impact on the static strength of the specimens. The failure modes of the specimens indicate that in static tensile tests, failure occurs at the non - welded positions, which is a typical necking ductile failure. In contrast, fatigue failure occurs at the welded spots and is a brittle failure.

(2) Stress amplitude and stress ratio are two crucial factors influencing the fatigue life. The greater the stress amplitude, the lower the fatigue life. At low stress amplitudes, the fatigue life exhibits higher sensitivity. As the stress ratio increases, the fatigue life decreases, the stress amplitude reduces, and the sensitivity of both the fatigue life and the stress amplitude to the stress ratio gradually increases.

(3) The fatigue S - N curve of the base metal indicates that the number of fatigue cycles decreases non - linearly as the stress amplitude increases. For a fatigue life of 2 million cycles, the stress amplitude of the base metal is approximately 230.16 MPa, while the stress amplitudes of specimens M1 - M5 range from 91.87 MPa to 194.03 MPa. Based on a survival rate of 97.7%, the modified stress amplitudes range from 81.19 MPa to 186.10 MPa, with an average value of 130.36 MPa. The overall stress amplitude of all specimens is 128.72 MPa. After correction, this value drops to 100.49 MPa, which is 45.75% lower than that of the base metal.

(4) The stress amplitude under ultra - high cycle loading is predicted. When the number of fatigue cycles exceeds 10 million, the stress amplitude drops below 80 MPa. After correction, it reaches 59.60 MPa. The coupling relationship among stress-amplitude, stress-ratio, and fatigue-cycle is fitted and analyzed, and the relevant formula is derived. A comparison between the two fitting methods is conducted. Finally, a safety line for stress-amplitude and stress-ratio is established.

Acknowledgments

This work was funded by the Science Research Project of Hebei Education Department (Grant No. ZD2022140) and the Natural Science Foundation in Hebei Province (Grant No. E2024202216).

References

[1] H.-B. Liu, S. Li, L. Xu, and Z.-B. Yu, “Identification of wheel-rail forces on high-speed railways based on physical model and hybrid recursive neural networks,” *Engineering Structures*, vol. 338, p. 120547, 2025.

[2] J.-J. Deng, H.-Y. Zhai, and Z.-J. Wang, “Vulnerability evaluation of high-speed railway network under wind disasters,” *Reliability Engineering and System Safety*, vol. 264(PA), p.111323, 2025.

[3] C.-F. Lu, J.-F. Liu, Y.-H. Liu, and Y.-M. Liu,“ Intelligent construction technology of railway engineering in China,” *Frontiers of Engineering Management*, vol.6,no.02,pp.503-516, 2019.

[4] T. Skriko, K. Lipiäinen, A. Ahola, H. Mettänen,and T. Björk, “Fatigue strength of longitudinal load-carrying welds in beams made of ultra-high-strength steel,” *Journal of Constructional Steel Research*, vol.179, p.106563, 2021.

[5] Z.-Y. Jie, W.-J. Wang, P. Zhuge, Y.-D. Li, and X. Wei, "Fatigue properties of inclined cruciform welded joints with artificial pits," *Advanced Steel Construction*,vol.17,no.01,pp. 20-27, 2021.
[6] A. Aloisio, D. Lavorato, J.-Q. Xue, J.-J. Wu, A. Rasulo, B. Briseghella, and C. Nuti, "The role of overstrength in welded joints for rebar substitution in damaged RC columns," *Construction and Building Materials*, vol.409, p.133952, 2023.
[7] Y.-Z. Jiang, Z.-Y. Xin, D.-Y. Wang, and T. Ou, "Structural fatigue performance of L-shaped support in continuous welded stainless steel roof system," *Journal of Constructional Steel Research*, vol.214, p.108507,2024.
[8] Q. Cheng, Z.-A. Yao, H.-Y. Chen, D.-W. Liu, M.-Y. Lin, Q. Zhao, and B. Zhang, "Study on corrosion fatigue degradation performance of welded top plate-U rib of cross-sea steel box girder," *Buildings*, vol.13, p.7, 2023.
[9] M. Gu, L.-W. Tong, X.-L. Zhao, and Y.-F. Zhang, "Numerical analysis of fatigue behavior of welded cfchs T-joint," *Advanced steel construction*, vol. 10, no. 04, pp. 476-496, 2014.
[10] H. Miao, T.Yamashita,K. Ushioda, S. Tsutsumi,Y. Morisada,and H. Fujii,"Improving fatigue property of linear friction welded cruciform joints of low carbon steel," *Journal of Manufacturing Processes*,vol.338,pp. 55-64, 2025.
[11] H.-L. Luo, K.-C. Qu, C. Yu, Q.-H. Kan, and G.-Z. Kang, "Experimental study on multiaxial ratchetting-fatigue interaction of SUS301L stainless steel tubular welded joint," *International Journal of Fatigue*, vol. 186, p.108411, 2024.
[12] W.- Z. Wang, Z.-Y. Jie, G. -J. Yu, L.- F. Xiao, and Y. -Z. Fan, "Unified fatigue life calculation of Q460c steel fillet weld cruciform joints considering fatigue crack initiation and propagation," *Advanced Steel Construction*, vol. 20, no. 03, pp. 222-231, 2024.
[13] Y.-F., Wang, W. Wang, and Y.-Q. Liu, "Experimental research on the fatigue performance of lapped welded splices of high strength reinforcing bars," *Journal of Railway Engineering Society*, vol. 38, no. 03, pp. 113-117, 2021.
[14] X.-W. Sheng, W.-Q. Zheng, and J.-Z. Lei, "Experimental study on fatigue behavior of high strength steel bars connected by flash butt welding in railway engineering," *China Civil Engineering Journal*, vol. 50,no. 12, pp. 56-61, 2017.
[15] W.-Q. Zheng, and X.-W. Sheng, "Welding properties for HRB500 high-strength steel bars connected by flash butt welding," *China Civil Engineering Journal*, vol. 52, no. 07, pp. 22-29, 2019.
[16] TB 10092-2017, "Code for the Design of Concrete Structures for Railway Bridges and Culverts," China Railway Publishing House Co., Ltd. 2017.
[17] GB 50010-2010, "Code for Design of Concrete Structures," China Construction Industry Press, 2016.
[18] M. Schwarzkopf, "Fatigue design of tack-welded mesh reinforcing bars," *Structural Engineering International*, vol. 5, no. 02, pp. 102-106, 1995.
[19] W.-L. Gu, and Z.-L. Lin, "Experimental research on fatigue properties of welded fabric," *Building Structure*, vol. 42, no. 01, pp. 105-107+90, 2012.
[20] W.-L. Gu, and A.-P. Zhu, "Experimental Research on Fatigue S-N Curves of Welded Fabric," *Construction Technology*, vol. 46, no. 04, pp. 71-74+103, 2017.
[21] C. Li, G.-S. Liu, and S.-Y. Wang, "Experimental Study on Fatigue Properties of Welded Steel Fabric," *Bulletin of Science and Technology*, vol. 38, no. 08, pp. 79-84,2022.
[22] JGJ 114-2014, "Technical specification for concrete structures reinforced with welded steel fabric," China Construction Industry Press, 2014.
[23] GB/T 28900-2022, "Test methods of steel for reinforcement of concrete," State Administration for Market Regulation, 2022.
[24] H. Esmaeili,M. Avateffazeli,M. Haghshenas,and R. Rizvi. "A Hybrid Framework for Characterizing and Benchmarking Fatigue S-N Curves in Aluminum Alloys by Integrating Empirical and Data-Driven Approaches,"*Fatigue & Fracture of Engineering Materials & Structures*, vol. 48,no. 1, pp. 44-59, 2024.
[25] M. Agrawal,M. Gupta,R T D. Prabhakaran, and P. Mahajan, "A comparative study of static and fatigue performance of glass and basalt fiber reinforced epoxy composites," *Polymer Composites,* vol. 45,no. 4, pp. 3551-3565, 2024.
[26] BS-EN 1993-1-9:2005, "Design of steel structures —Part 1-9: Fatigue,"U.K.: GEN, 2005.
[27] W.-Z. Yao, X.-W. Li, P.-S. Dong, "Fatigue-resistant design theory and method for welded structures," China Machine Press, 2017.
[28] JGJ/T 27-2014, "Standard for test methods of welded joint of reinforcing steel bars," China Construction Industry Press,2014.
[29] CEN. EN 1992-1-1. "Eurocode 2: Design of concrete structures—Part 1–1: general rules and rules for buildings," European Committee for Standardization, Brussels, 2004.
[30] DIN 1045-1, "Tragwerke aus Beton, Stahlbeton und Spannbeton Teil 1: Bemessung und Konstruktion," 2008.
[31] J.-X. Wen, H.-J. Li, F.-L. Huang, Z.-Q. Yang, Z. Wang, and Z.-L. Yi, "Fatigue Performance Test System for Ballastless Track Concrete of High Speed Railway," *Railway Engineering*, vol. 62, no. 12, pp. 7-11, 2022.
[32] J.-W. Zhang, C.-B. Cai, S.-Y. Zhu, M.-Z. Wang, Q.-L. He, S.-F. Yang, and W.-M. Zhai, "Experimental investigation on dynamic performance evolution of double-block ballastless track under high-cycle train loads," *Engineering Structures*, vol. 254, p. 113872, 2022.